The British Journal of Radiology, 83 (2010), 831–840

Venous structures at the craniocervical junction: anatomical variations evaluated by multidetector row CT

[1]S TANOUE, MD, [1]H KIYOSUE, MD, [1]Y SAGARA, MD, [2]Y HORI, MD, [3]M OKAHARA, MD, [3]J KASHIWAGI, MD and [1]H MORI, MD

[1]*Department of Radiology, Oita University Faculty of Medicine, Idaigaoka 1-1, Hasama-machi, Yufu-shi, Oita, 879–5593, Japan,* [2]*Nagatomi Neurosurgical Hospital, Nishi-Ohmichi, 2-1-20, Oita-shi, Oita, 870-0820, Japan and* [3]*Department of Radiology, Shinbeppu Hospital, Tsurumi, 3898, Beppu-shi, Oita, 874-0833, Japan*

ABSTRACT. The aim of this study was to evaluate the anatomy of and normal variations in the craniocervical junction veins. We retrospectively reviewed 50 patients who underwent contrast-enhanced CT with a multidetector scanner. Axial and reconstructed images were evaluated by two neuroradiologists with special attention being paid to the existence and size of veins and their relationships with other venous branches around the craniocervical junction. The venous structures contributing to craniocervical junction venous drainage, including the inferior petrosal sinus (IPS), transverse-sigmoid sinus, jugular vein, condylar vein, marginal sinus and suboccipital cavernous sinus were well depicted in all cases. The occipital sinus (OS) was identified in 18 cases, including 4 cases of prominent-type OS. The IPS showed variations in drainage to the jugular vein through the jugular foramen or intraosseous course of occipital bone via the petroclival fissure. In all cases, the anterior condylar veins connected the anterior condylar confluence to the marginal sinus; however, a number of cases with asymmetry and agenesis in the posterior and lateral condylar veins were seen. The posterior condylar vein connected the suboccipital cavernous sinus to the sigmoid sinus or anterior condylar confluence. The posterior condylar canal in the occipital bone showed some differences, which were accompanied by variations in the posterior condylar veins. In conclusion, there are some anatomical variations in the venous structures of the craniocervical junction; knowledge of these differences is important for the diagnosis and treatment of skull base diseases. Contrast-enhanced CT using a multidetector scanner is useful for evaluating venous structures in the craniocervical junction.

Received 31 May 2009
Accepted 14 July 2009

DOI: 10.1259/bjr/85248833

Intracranial veins and venous sinuses converge to form major dural sinuses, the transverse sinus and the sigmoid sinus, which drain into extracranial veins. These major dural sinuses are connected by other venous structures at the skull base. These venous structures form complex venous networks that drain intracranial venous flow into extracranial veins at the craniocervical junction [1]. These venous structures are also known to have an important role as collateral pathways in cases of venoocclusive disease. The typical relationships between the craniocervical junction veins are shown in Figure 1. Knowledge of the anatomical relationships and variations of these veins is necessary not only for radiological diagnosis, but also when considering surgical or endovascular treatment of skull base diseases. Some investigators have previously reported the anatomy of and variations in these veins using anatomical and radiological methods with conventional angiography or contrast-enhanced MRI [2–8]. CT has been recognised as inadequate for evaluations of the posterior fossa owing to artefacts from bony structures; however, recent applications of multidetector row CT (MDCT) enable us to evaluate the posterior fossa with thin-sectional axial images and/or three-dimensional reconstructed images. In this study, the venous structures at the craniocervical junction were evaluated using 32-channnel MDCT, focusing on anatomical variations.

Address correspondence to: Shuichi Tanoue, MD, Department of Radiology, Oita University Faculty of Medicine, Idaigaoka, 1-1, Hasama-machi, Yufu-shi, Oita 879-5593, Japan. E-mail: stanoue@med.oita-u.ac.jp

Methods and materials

Imaging technique

A multislice CT scanner with a 32-channel detector (Aquillion 32; Toshiba Medical Systems, Tokyo, Japan) was used for contrast-enhanced CT. The scan area ranged from the top of the cranium to the second cervical vertebra parallel to the orbitomeatal line. The imaging parameters were as follows: 24 cm field of view (FOV), 120 kVp, 300 mA, 512×512 matrix size, 20 helical pitch, 0.5 s per rotation and 40 mm s^{-1} table speed. Helical scanning was started 60 s after the intravenous administration of a non-ionic iodine-containing contrast agent (300 mg ml^{-1}, 100 ml). The obtained axial data were reconstructed at 0.5 or 1 mm thicknesses and then transferred to a separate workstation (AquariusNetStation; Teraricon Inc. San Mateo, CA) on which three-dimensional surface rendering and multiplanar reconstruction were available.

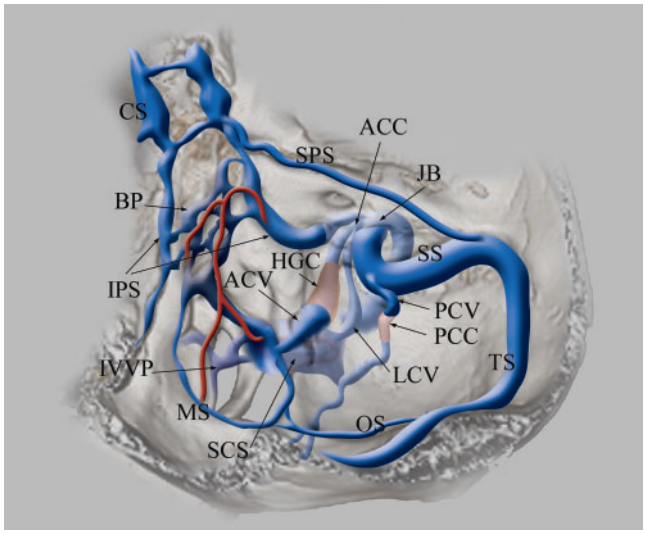

Figure 1. Schematic drawing of the veins at the craniocervical junction. The inferior petrosal sinus (IPS) originates from the posterosuperior aspect of the cavernous sinus (CS), runs along the petroclival fissure and drains into the jugular bulb (JB). Basilar plexus (BP) lies on the clivus with connecting bilateral IPS. The anterior condylar vein (ACV) and lateral condylar vein (LCV) originate from the medial aspect of the JB, forming an anterior condylar confluence (ACC). ACV runs medially through the hypoglossal canal (HGC) and drains into the lateral part of the marginal sinus (MS). MS is contiguous to the medial part of the suboccipital cavernous sinus (SCS). LCV runs posterolaterally and flows into SCS. The posterior condylar vein (PCV) originates from the sigmoid sinus (SS), runs through the posterior condylar canal (PCC) and flows into SCS. SCS lies under the occipital bone surrounding the horizontal portion of the vertebral artery. The occipital sinus (OS) originates from the torcular herophili, confluence of transverse sinus (TS) and straight sinus and drains into the posterior part of MS. MS is the round-shaped sinus surrounding the foramen magnum. MS and the medial part of SCS are connected to the internal vertebral venous plexus (IVVP).

Patients

The study was approved by the institutional review board. Consecutive adult patients who underwent contrast-enhanced CT between March 2006 and January 2007 were retrospectively evaluated. Patients who had venoocclusive disease in the craniocervical junction owing to tumours or other pathological conditions were excluded; 100 sides from the remaining 50 patients (27 men and 23 women; age range 20–92 years; mean age 63 years) were investigated. The underlying diseases or objectives of examination in these patients were malignant tumours of the body trunk in 14, head and neck tumours in 13, brain tumours in 5, cerebral haemorrhage in 4 and screening examinations in 14 cases.

Evaluation

The images obtained were independently evaluated by two neuroradiologists (TS and KH) on the workstation by paging through the source images and/or making a three-dimensional reconstruction in an identical window parameter. Veins at the craniocervical junction, including the inferior petrosal sinus (IPS), marginal sinus (MS), suboccipital cavernous sinus (SCS), occipital sinus (OS), anterior condylar vein (ACV), lateral condylar vein (LCV), posterior condylar vein (PCV) and anterior condylar confluence (ACC), were investigated. The analysis focused on several key areas: the detectability of each vein, the location and course of the veins and connections with surrounding veins and the transverse diameters of the tubular venous structures. The SCS, previously termed by Arnautović et al [9], is a venous structure lying under the occipital bone with surrounding vertical part of vertebral artery. The ACC is described by San Millán Ruítz et al [1] as a venous structure merging IPS, ACV and LCV into a jugular bulb. Among the venous structures, veins that presented tubular configurations (IPS, OS and the vertical extracanalicular portion of ACV, LCV and PCV) and jugular bulbs were targeted for measurements of their diameters. These tubular veins were measured at the largest diameters of the minimum axis on transverse images. Moreover, each measurement was evaluated for statistical correlation with measurements of the ipsilateral veins to evaluate the asymmetry and relationships of the veins.

Results

Detectability

The IPS, MS, SCS and ACV were identified on transverse images and three-dimensional surface images in all 100 sides (100%) from 50 cases. The OS was identified in only 18 cases (36%). The LCV was identified in 73 sides (73%) and the PCV was identified in 67 sides (67%).

Distribution

The draining pattern of IPS presented two variations, Type A and Type B. In Type A, the IPS originates at the posterosuperior aspect of the cavernous sinus, runs along the petroclival fissure and drains into the medial part of the jugular bulb through the anterior edge of the jugular foramen (Figure 2). In Type B, the IPS runs along the petroclival fissure, penetrates the mid-portion of the petroclival fissure and drains into the medial part of the jugular bulb. Type A IPS was seen in 92 sides (92%) and Type B was seen in 8 sides (8%). Among Type B, in six sides (6%) the IPS flowed directly into the jugular bulb (Type B_1, Figure 3); in the remaining two sides (2%), the IPS joined the proximal segment of the inferior petroclival vein (Type B_2, Figure 4).

The MS was identified as a circular venous structure lying along the foramen magnum in all cases (Figure 5). The SCS was identified as a venous plexus surrounding the horizontal portion of the vertebral artery at the craniocervical junction in all cases (Figure 5). All four prominent types of OS originate from the torcular herophili, run along the internal occipital crest and flow into the right sigmoid sinus (Figure 6). Other types of OS drained into the marginal sinus in seven cases and the sigmoid sinus in three cases. The caudal connection of the remaining four cases could not be demonstrated.

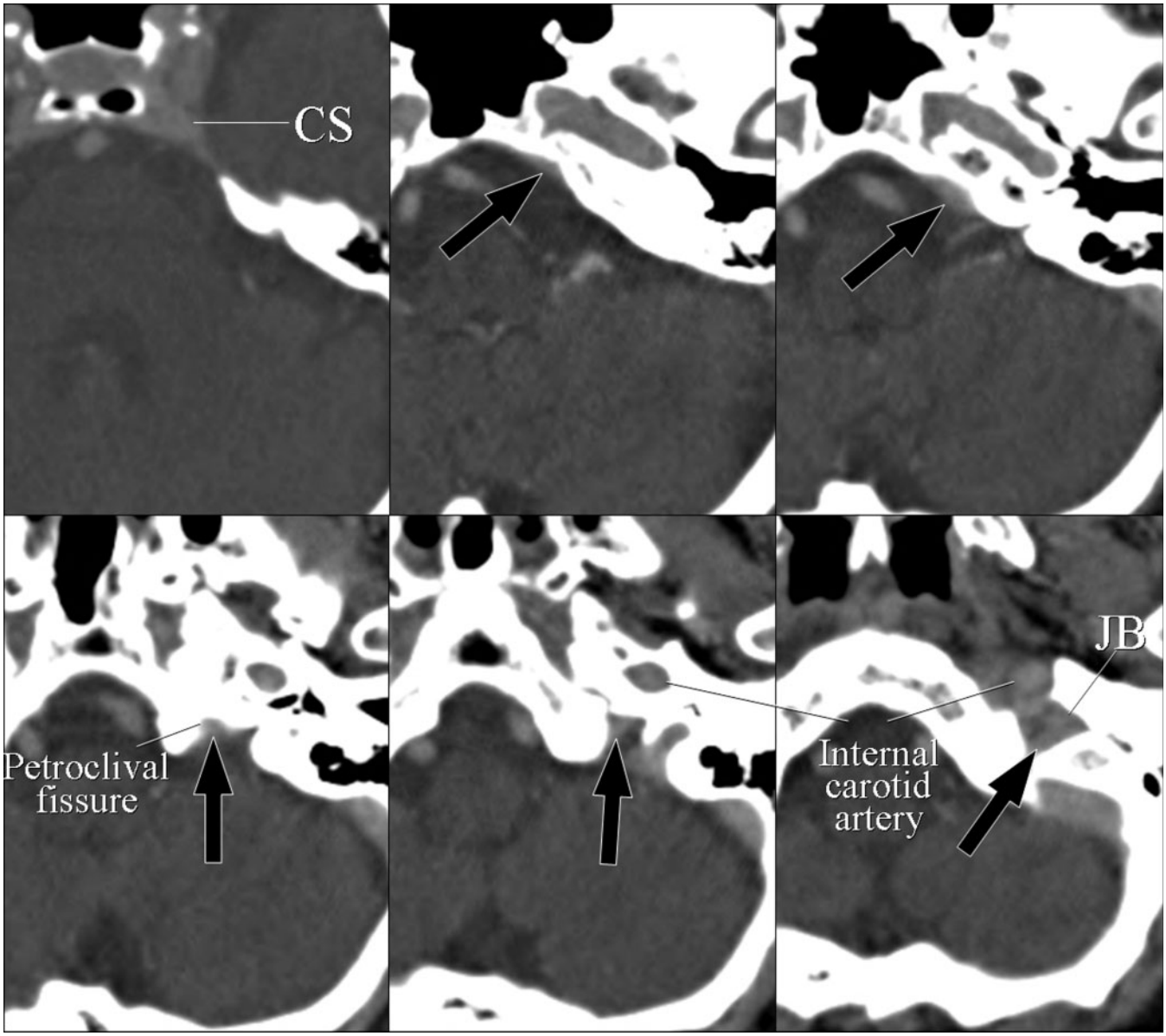

Figure 2. Type A inferior petrosal sinus (IPS). A 79-year-old female with lung cancer. Axial CT images showing the IPS (black arrows), which originates from the posterosuperior part of the cavernous sinus (CS), runs along the petroclival fissure and drains into the jugular bulb (JB).

The ACV originates from the anterior condylar confluence (ACC), runs through the hypoglossal canal forming a venous plexus and drains into the marginal sinus in all sides (Figure 5). The LCV originates from ACC, runs along the extracranial aspect of the occipital condyle and drains into the anterolateral portion of the SCS in all sides (Figure 5). The PCV presented three anatomical variations [1]: the PCV originates from the inferomedial aspect of the sigmoid sinus, runs within the occipital bone forming a posterior condylar foramen and drains into a posterior portion of the SCS (Type A, Figure 5) [2]; the posterior condylar canal is exposed to the intracranial surface of the occipital bone (Type B, Figure 7); or [3] the PCV originates from the ACC and drains into the SCS (Type c, Figure 8). A Type A PCV was seen in 50 out of 67 sides (75%), Type B was seen in 14 sides (21%) and Type C was seen in three sides (4%).

Diameters of the connecting veins

The measured diameters of the venous structures are summarised in Table 1. These data demonstrate wide variance. There was a statistically significant asymmetry of the size of the jugular bulb.

The coefficients of correlation between the measurements of the veins and their ipsilateral connecting veins are shown in Table 2. The coefficients in several relationships were investigated: IPS and jugular bulb; ACV and LCV, PCV and jugular bulb; LCV and PCV and jugular bulb; and PCV and jugular bulb. Among these relationships between the diameters of the connecting veins, the two relationships of PCV and LCV showed a strong negative correlation. The two relationships that presented a strong negative correlation are shown in Figure 9 as scatter diagrams. OS was excluded from this analysis because of the small number of depictions on MDCT.

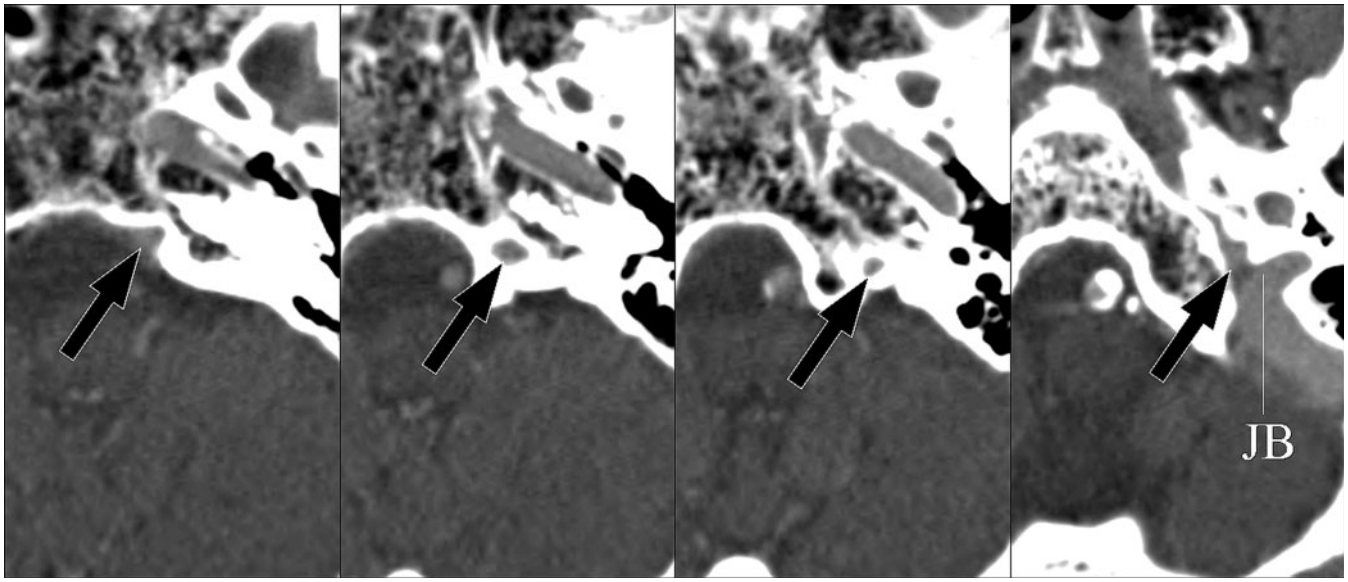

(a)

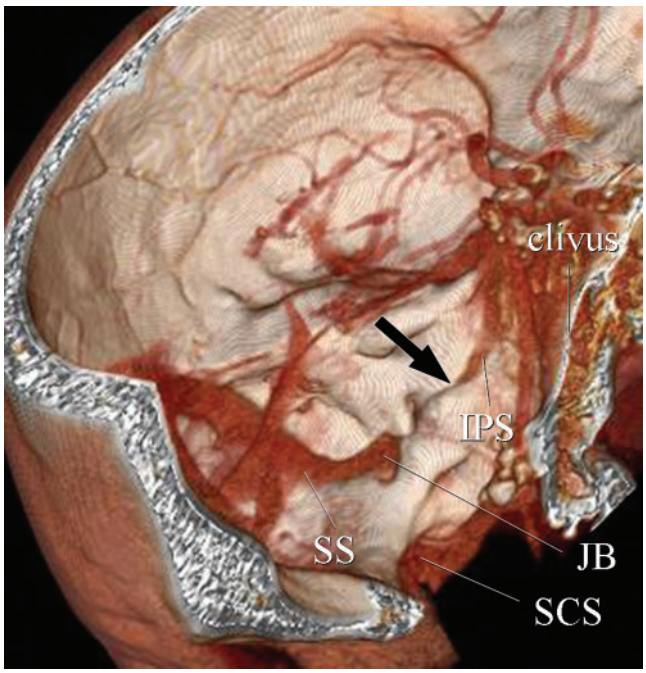

(b)

Figure 3. Type B_1 inferior petrosal sinus (IPS). A 92-year-old male with burn injury of the scalp. (a) Axial CT images show the left IPS, which runs along with and penetrates the occipital bone through the petroclival fissure, draining into the jugular bulb (JB) (arrows). (b) Three-dimensional surface rendering image demonstrates impaction of the distal part of the left IPS within the occipital bone (arrow). SCS, suboccipital cavernous sinus; SS, sigmoid sinus.

Discussion

The craniocervical junction is an anatomically critical area where the brain stem, several cranial nerves, arteries and veins exist in a restricted space. The venous structures include the major dural sinuses and emissary veins that have a role as the main drainage route for cephalic venous blood flow. The emissary veins are also thought to have a function of redirecting blood outflow towards the vertebral venous system in the upright position [10]. These venous structures communicate with each other to form complex venous networks and present some variations in their connection patterns.

Previous radiological studies of the anatomy and/or variations of craniocervical venous structures have been carried out using transcatheter angiography or MRI [2–8]. Takahashi et al [7] evaluated the venous anatomy around the SCS using contrast-enhanced MRI with three-dimensional fast spoiled gradient-recalled acquisition in the steady state (3D-SPGR) with fat suppression; all venous structures could be clearly depicted. Contrast-enhanced three-dimensional fast gradient-echo MRI has the advantage of depicting skull base venous structures because of

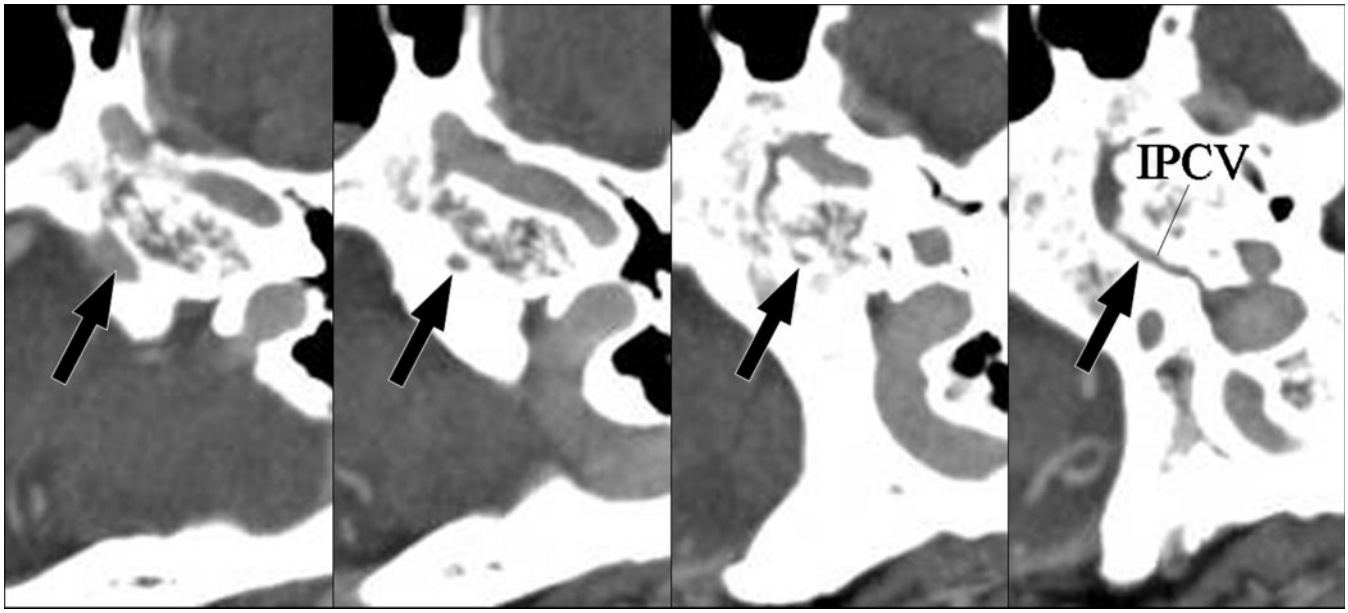

Figure 4. Type B_2 inferior petrosal sinus (IPS). A 79-year-old female with tinnitus. Axial CT images show the left IPS penetrating the petroclival bone and draining into the inferior petroclival vein (arrows).

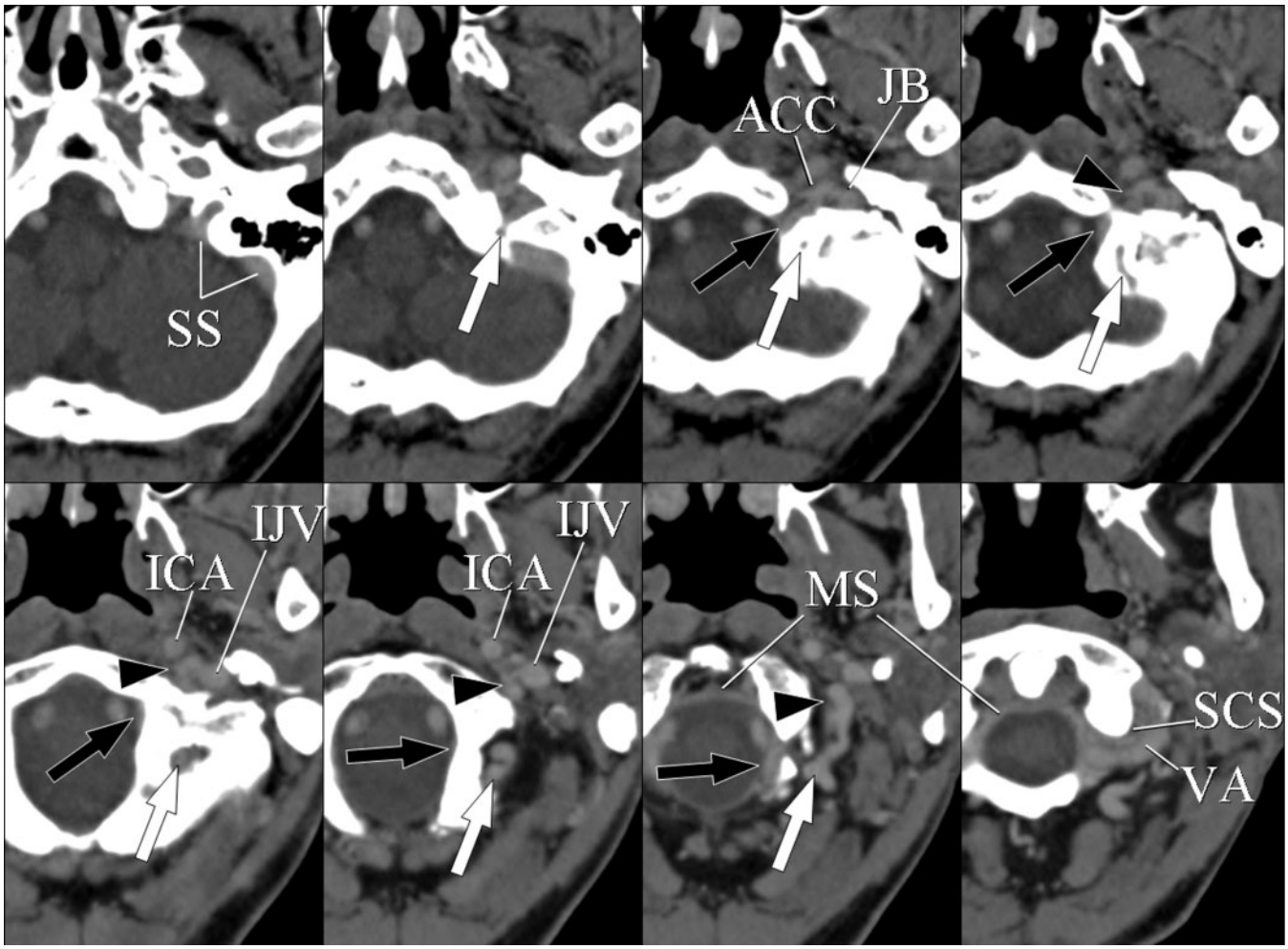

Figure 5. A 74-year-old female with cerebral cavernous hemangioma. Axial CT images show the anterior condylar vein (ACV), lateral condylar vein (LCV), posterior condylar vein (PCV), marginal sinus (MS), suboccipital cavernous sinus (SCS) and their connections. The ACV originates from anterior condylar confluence (ACC) and passes through the hypoglossal canal. The ACV then descends along the intracranial surface of the occipital bone and drains into the MS (black arrows). The MS is shown as a circular venous structure along the foramen magnum. The SCS is a venous plexus surrounding the horizontal vertebral artery (VA). The LCV originates from the ACC and runs posterolaterally to join the SCS (arrowheads). The PCV originates from the sigmoid sinus (SS), runs downwards through the posterior condylar canal and drains into the SCS (white arrows). IJV, internal jugular vein; ICA, internal carotid artery; JB, jugular bulb.

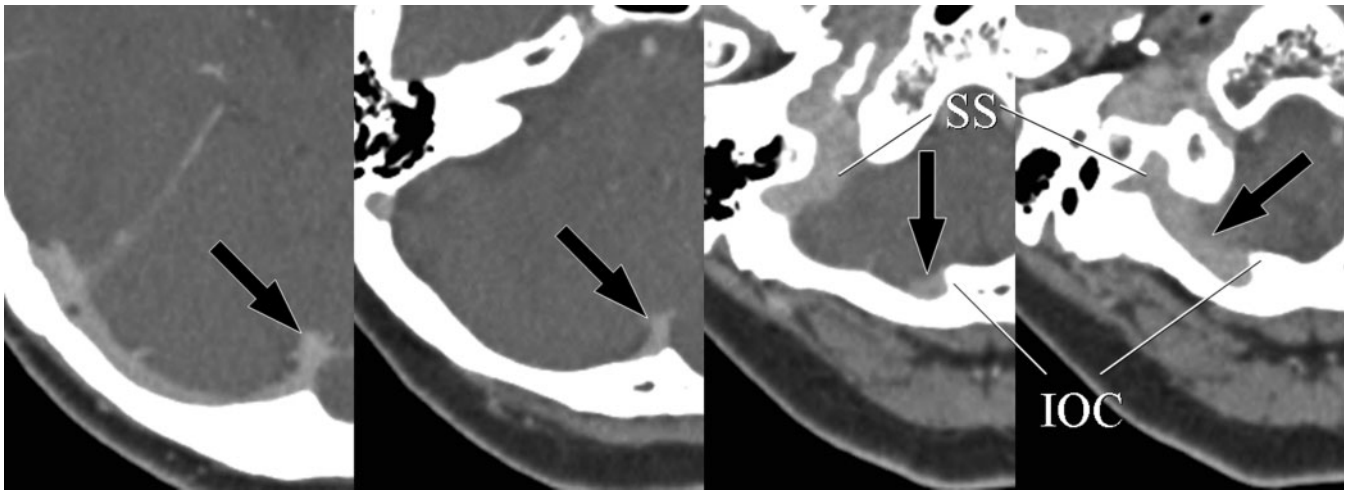

(a)

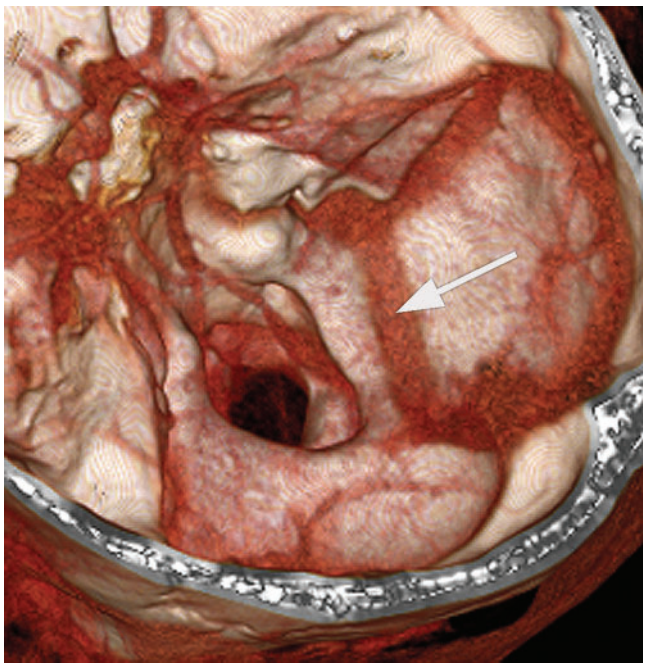

(b)

Figure 6. A 66-year-old female with malignant melanoma of the upper extremity. (a) Axial CT images show occipital sinus (OS) originating from the torcular herophili and running along the internal occipital crest (IOC) (arrows). OS drains into the right sigmoid sinus (SS) without connection to the marginal sinus. This image indicates the prominent type of OS. (b) This three-dimensional reconstructed image shows a prominent type of OS draining into the right sigmoid sinus (arrow).

its high resolution between veins and bones [11]. There are also some previous reports evaluating posterior fossa veins using conventional CT; however, these investigations have been performed only with a bony algorithm [6, 12, 13]. Recently, the development of MDCT has enabled the demonstration of intracranial as well as skull base vessels, because it provides higher spatial and temporal resolution.

In our study, the IPS, SCS, MS and ACV could be depicted in all cases, even if passing adjacent to or through bony structures. The anatomical architectures of the LCV and PCV could be evaluated; the LCV was found to be absent in 27 sides (27%) and the PCV was absent in 33 sides (33%). These results presented a similar frequency to the results of a previous study [7]. The OS was depicted in only 18 cases, with 4 cases of prominently developed OS. There is an apparent discrepancy between our results and those of a previous anatomical study, which presented the frequency of absence of the OS as 35.5% [14]. This could be because the resolution of an MDCT image is not sufficient to depict the normal OS, which is the smallest dural sinus in the cranium, and because the OS runs along the internal occipital crest, which has a thick and prominent bony cortex.

The IPS normally connects the cavernous sinus to the jugular bulb and passes along the petroclival fissure. There are many reports evaluating the anatomy of, and variations in, the IPS using transcatheter venography [2–5]. Most investigators have classified the IPS in the context of

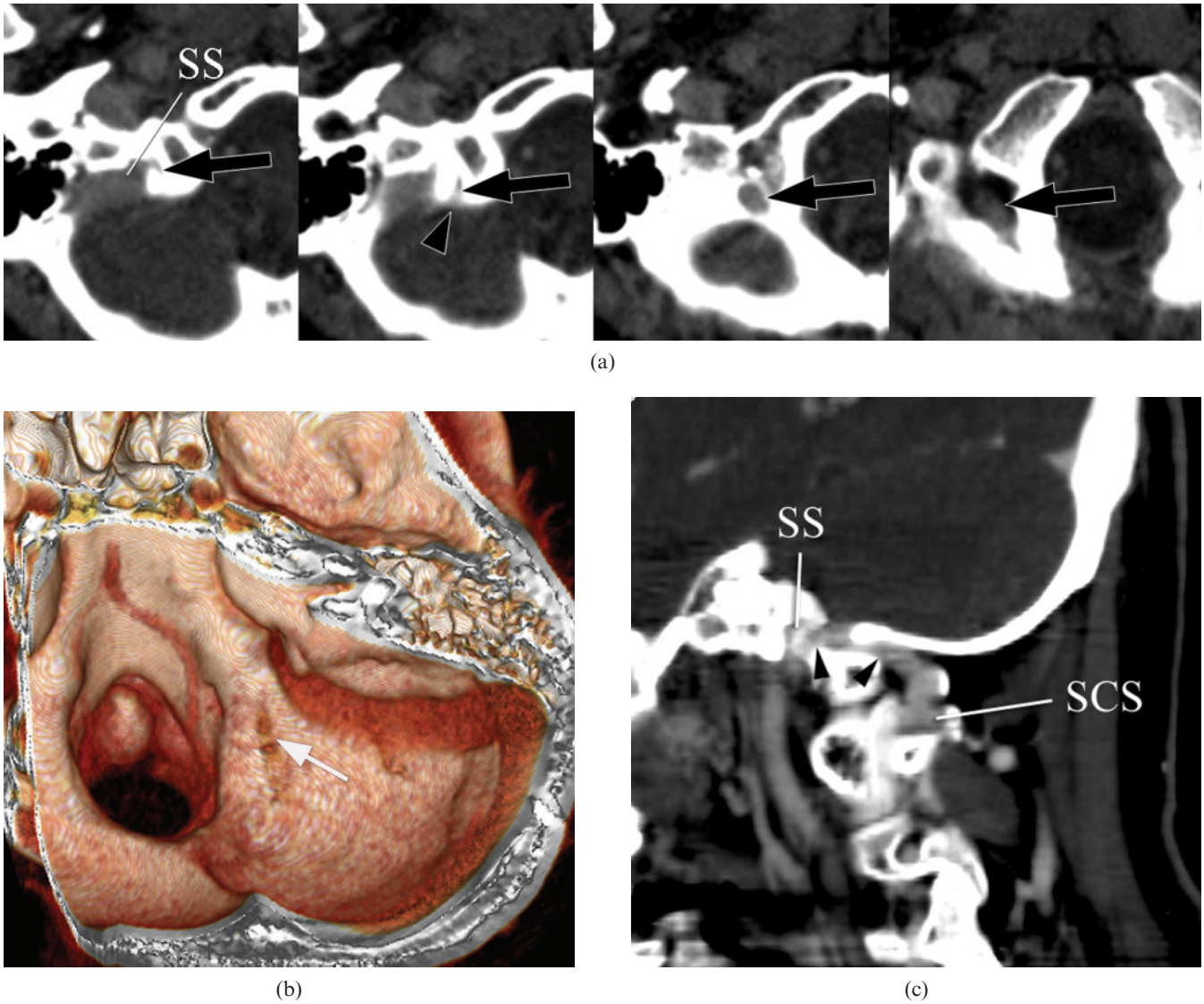

Figure 7. A 43-year-old male with malignant glioma. (a) Axial CT images show the posterior condylar vein (PCV) running through the posterior condylar canal (arrows). The posterior condylar canal is exposed at the intracranial surface of the occipital bone (arrowhead). (b) This three-dimensional reconstructed image shows the posterior condylar canal exposed at the intracranial surface of the occipital bone (arrow). (c) The PCV is demonstrated continuously on this oblique sagittal multiplanar reconstruction image (arrowheads). SCS, suboccipital cavernous sinus; SS, sigmoid sinus.

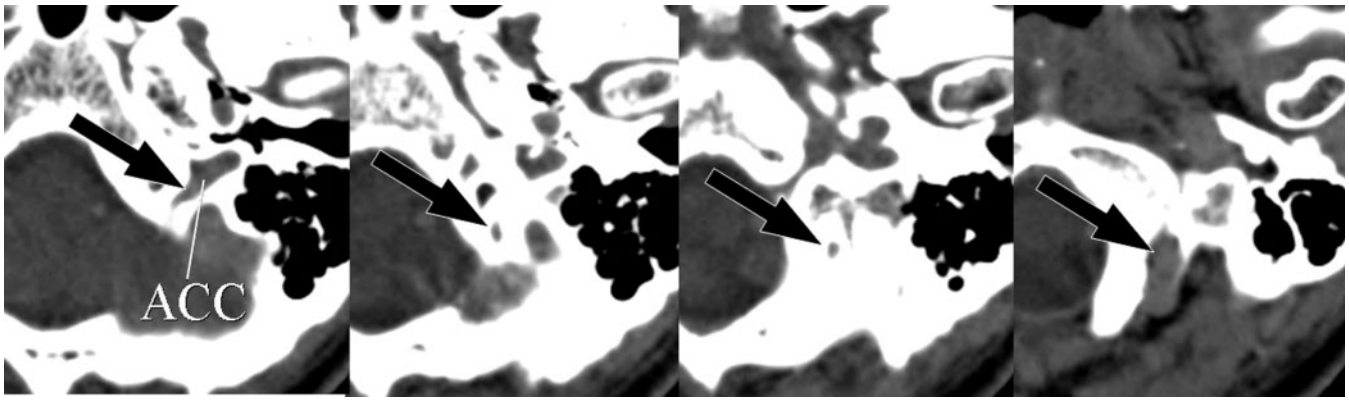

Figure 8. A 59-year-old female with intracerebral haemorrhage. Axial CT images show the posterior condylar vein originating from the anterior condylar confluence (ACC) and draining into the suboccipital cavernous sinus through the posterior condylar canal (arrows).

Table 1. Calculated diameters of the veins

Vein		Diameter (mm)	Mean (mm)	Significance[a]
IPS	Right	1.0–3.7	0.99	$p=5551$
	Left	1.0–3.5	2.04	
OS		4.0–5.3	4.7	
ACV	Right	1.0–5.3	3.03	$p=0.0846$
	Left	1.4–5.5	3.24	
LCV	Right	1.0–6.6	3.75	$p=0.937$
	Left	1.6–5.8	3.43	
PCV	Right	2.2–6.7	4.17	$p=0.3373$
	Left	1.8–8.4	3.93	
JB	Right	4.5–11.7	6.94	$p<0.0001$
	Left	3.3–11.0	5.50	

[a]Paired *t*-test. IPS, inferior petrosal sinus; OS, occipital sinus; ACV, anterior condylar vein; LCV, lateral condylar vein; PCV, posterior condylar vein; JB, jugular bulb.

the patterns of the IPS–jugular bulb junction, for example single or multiple connections, plexiform connection, no connection or connection with cervical venous plexus. Although our cases could not be evaluated with regards to the connection pattern by MDCT, there were some variations in the route passing through the petroclival fissure. CT images have the advantage of being able to depict the relationship between bones and veins. Furthermore, the penetration of the IPS from the intracranial surface into the bone was demonstrated spatially on three-dimensional surface reconstructions.

The OS could be demonstrated in prominently developed cases and all drained into the right sigmoid sinus. According to a previous anatomical description, the number of OS running towards the right side is three times larger than the number of OS going to the left [15], consistent with our results. By contrast, there was no variation in the configuration of the SCS and the marginal sinus.

Most PCVs originated from the inferolateral aspect of the sigmoid sinus in our study; there were three cases of a PCV originating from the ACC. San Millán Ruítz et al [1] reported that the PCV in 11 of 12 cases originated from the jugular bulb and only one originated from the sigmoid sinus, in contradiction to our results. Thus, there was a discrepancy in the results, although the number of patients was different. Further investigations in larger populations are necessary. In our study by MDCT, there were two variations in the posterior condylar canal in terms of the pattern of passing through the occipital bone: one passes from the sigmoid fissure to the occipital condyle through the occipital bone, forming an entire canal, whereas the other passes through the occipital bone and is exposed to the intracranial surface. The latter pattern could be spatially observed on three-dimensional surface images. There was no variation in the running patterns of the anterior condylar or lateral condylar veins in our study.

Table 2. Coefficients of correlation between measurements of veins and ipsilateral connecting veins

Relationship	Coefficients[a]	Significance level[a]	
		5%	1%
IPS–JB	Rt $r=-0.08509$	NC	NC
	Lt $r=0.035468$	NC	NC
ACV–LCV	Rt $r=0.058341$	NC	NC
	Lt $r=0.064815$	NC	NC
ACV–PCV	Rt $r=0.077843$	NC	NC
	Lt $r=0.389071$	C	C
ACV–JB	Rt $r=-0.075079$	NC	NC
	Lt $r=0.111958$	NC	NC
LCV–PCV	Rt $r=-0.672805$	C	C
	Lt $r=-0.490995$	C	C
LCV–JB	Rt $r=0.155963$	NC	NC
	Lt $r=0.267303$	NC	NC
PCV–JB	Rt $r=-0.229727$	NC	NC
	Lt $r=-0.266212$	NC	NC

[a]Spearman's coefficient by rank. IPS, inferior petrosal sinus; ACV, anterior condylar vein; LCV, lateral condylar vein; PCV, posterior condylar vein; JB, jugular bulb; Rt, right; Lt, left; C correlated; NC, not correlated.

The numbers of each measurement varied appreciably depending on the veins and sides measured. Among them, there was a statistically significant asymmetry in the diameters of jugular bulbs. Okudera et al [16] described that asymmetry of the jugular bulb could occur owing to negative pulse waves from the right cardiac atrium to the right jugular bulb, through the straight right internal jugular vein. Our result, showing significant asymmetry, is reflected by embryological consideration of the asymmetry of the jugular bulb. The relationships among the ipsilateral connecting veins only showed a strong negative correlation in bilateral PCL–LCV analysis. This result suggests that the LCV and PCV develop and function complementarily, and that they are important drainage veins from the sigmoid sinus/jugular bulb to the cervical venous plexus. Furthermore, the left ACV and PCV were only weakly correlated. The reason why they had this statistical correlation cannot be explained; again, further investigation in a larger population is necessary.

These variations have various clinical significances. The IPS is the most frequent route through which to approach the cavernous sinus in endovascular treatment for cavernous arteriovenous shunt or for venous sampling for the diagnosis of microadenoma in the pituitary gland; therefore, understanding its anatomical variations is important for catheterisation to the IPS and the cavernous sinus. The OS and condylar veins function as collateral pathways in venoocclusive diseases, and neurosurgeons need to pay careful attention to

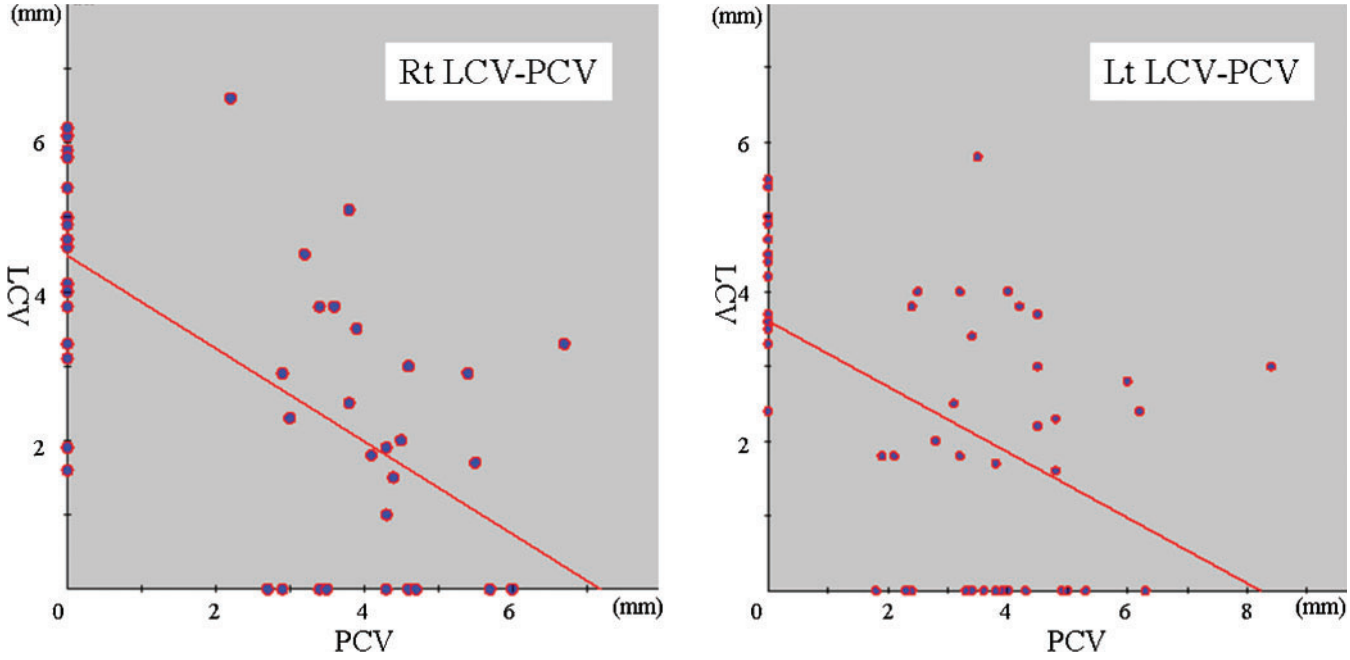

Figure 9. Scatter diagrams of the relationships between the bilateral posterior condylar vein (PCV) and lateral condylar vein (LCV). This diagram of the diameters of these two veins in each case reveals strong negative correlations. Lt, left; Rt, right.

suboccipital craniotomy. Contrast-enhanced MDCT images are useful, especially in evaluating the relationships between craniocervical junction veins and bony structures. The condylar veins can also be used as access routes to hypoglossal dural arteriovenous fistulas [17] and transverse-sigmoid dural arteriovenous fistulas with occlusion of the jugular vein. Furthermore, dural arteriovenous fistulas can involve the condylar veins [18]. Thus, understanding their normal anatomy and variations is of clinical importance when considering endovascular treatments for posterior fossa dural arteriovenous fistulas.

Conclusion

The venous structures at the craniocervical junction showed several anatomical variations. In particular, the IPS, OS, PCV and LCV demonstrate variations in their existence, size and communication with other veins. These structures were well depicted and it was possible to evaluate their anatomy and variation on axial and three-dimensional reconstructed images using an MDCT. These images are useful in evaluations of the relationships between veins and bones.

Acknowledgements

The authors gratefully acknowledge the co-operation of the radiological technologists Y Murakami and T Shiroo for their help in optimal imaging.

References

1. San Millán Ruítz D, Gailloud P, Rufenacht DA, Delavelle J, Henry F, Fasel JH. The craniocervical venous system in relation to cerebral venous drainage. AJNR Am J Neuroradiol 2002;23:1500–8.
2. Shiu PC, Hanafee WN, Wilson GH, Rand RW. Cavernous sinus venography. Am J Roentgenol Radium Ther Nucl Med 1968;104:57–62.
3. Theron J, Djindjian R. Cervicovertebral phlebography using catheterization. Radiology 1973;108:325–31.
4. Doppman JL, Oldfield E, Krudy AG, Chrousos GP, Schulte HM, Schaaf M, et al. Petrosal sinus sampling for Cushing syndrome: anatomical and technical considerations. Work in progress. Radiology 1984;150:99–103.
5. Miller DL, Doppman JL, Chang R. Anatomy of the junction of the inferior petrosal sinus and the jugular vein. AJNR Am J Neuroradiol 1993;14:1075–83.
6. Gebarski SS, Gebarski KS. Inferior petrosal sinus: imaging – anatomic correlation. Radiology 1995;194:239–47.
7. Takahashi S, Sakuma I, Omachi K, Otani T, Tomura N, Watarai J, et al. Craniocervical venous anatomy around the suboccipital cavernous sinus: evaluation by MR imaging. Eur Radiol 2005;15:1694–700.
8. Caruso RD, Rosenbaum AE, Chang JK, Joy SE. Craniocervical junction venous anatomy on enhanced MR images: the suboccipital cavernous sinus. AJNR Am J Neuroradiol 1999;20:1127–31.
9. Arnautović KI, al-Mefty O, Pait TG, Krisht AF, Husain MM. The suboccipital cavernous sinus. J Neurosurg 1997; 86:252–62.
10. Valdueza JM, von Münster T, Hoffman O, Schreiber S, Einhäupl KM. Postural dependency of the cerebral venous outflow. Lancet 2000;355:200–1.
11. Tanoue S, Kiyosue H, Hori Y, Sagara Y, Hori Y, Kashiwagi J, et al. Paracavernous sinus venous structures: anatomic variations and pathologic conditions evaluated on fat-suppressed 3D fast-gradient-echo MR images. AJNR Am J Neuroradiol 2006;27:1083–9.
12. Ginsberg LE. The posterior condylar canal. AJNR Am J Neuroradiol 1994;15:969–72.
13. Weissman JL. Condylar canal vein: unfamiliar normal structures as seen at CT and MR imaging. Radiology 1994;190:81–4.

14. Das AC, Hasan M. The occipital sinus. J Neurosurg 1970;33:307–11.
15. Hacker H. Dural venous sinuses. In: Newton TM, Potts DG, editors. Radiology of the skull and brain. Vol 2 Book 3 Veins. Saint Louis, Mo: CV Mosby, 1974: 1862–72.
16. Okudera T, Huang YP, Ohta T, Yokota A, Nakamura Y, Maehara F et al. Development of posterior fossa dural sinuses, emissary veins, and jugular bulb: morphological and radiologic study. AJNR Am J Neuroradiol 1994;15:1871–83.
17. Kiyosue H, Hori Y, Okahara M, et al. Dural arteriovenous fistula involving the hypoglossal canal: case reports and literature review. 8th World Federation of Interventional and Therapeutic Neuroradiology. 2005, Oct 19–22; Venice, Abstract. Interventional Neuroradiology 2005;11:Suppl 2:127.
18. Kiyosue H, Okahara M, Sagara Y, Tanoue S, Ueda S, Mimata C, et al. Dural arteriovenous fistula involving the posterior condylar canal. AJNR Am J Neuroradiol 2007;28:1599–601.